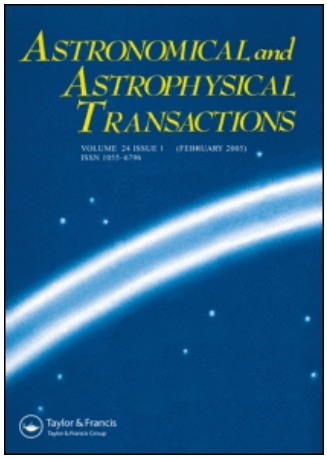

Astronomical & Astrophysical Transactions
The Journal of the Eurasian Astronomical Society
Publication details, including instructions for authors and subscription information:
http://www.informaworld.com/smpp/title~content=t713453505

Radio-sounding observations of a coronal mass ejection during the Galileo solar conjunction in January 1997

A. I. Efimov [a]; L. N. Samoznaev [a]; V. K. Rudash [a]; I. V. Chashei [b]; M. K. Bird [c]; D. Plettemeier [d]
[a] Institute of Radio Engineering & Electronics, Russian Academy of Sciences, Moscow, Russia
[b] Lebedev Physical Institute, Russian Academy of Science, Moscow, Russia
[c] Argelander-Institute für Astronomie, University of Bonn, Bonn, Germany
[d] Technische University of Dresden, Elektrotechnisches Institute, Dresden, Germany

Online Publication Date: 01 December 2007
To cite this Article: Efimov, A. I., Samoznaev, L. N., Rudash, V. K., Chashei, I. V., Bird, M. K. and Plettemeier, D. (2007) 'Radio-sounding observations of a coronal mass ejection during the Galileo solar conjunction in January 1997', Astronomical & Astrophysical Transactions, 26:6, 455 - 465
To link to this article: DOI: 10.1080/10556790701595210
URL: http://dx.doi.org/10.1080/10556790701595210

Astronomical and Astrophysical Transactions
Vol. 26, No. 6, December 2007, 455–465

Radio-sounding observations of a coronal mass ejection during the Galileo solar conjunction in January 1997

A.I. EFIMOV†, L.N. SAMOZNAEV†, V.K. RUDASH†, I.V. CHASHEI‡, M.K. BIRD§ and D. PLETTEMEIER#

†Institute of Radio Engineering & Electronics, Russian Academy of Sciences, 125009 Moscow, Russia
‡Lebedev Physical Institute, Russian Academy of Science, 117924 Moscow, Russia
§Argelander-Institute für Astronomie, University of Bonn, 53121 Bonn, Germany
#Technische University of Dresden, Elektrotechnisches Institute, 01062 Dresden, Germany

(Received 19 July 2007)

Frequency and amplitude fluctuations of the Galileo S-band radio signal were recorded nearly continuously during the spacecraft's solar conjunction from December 1996 to February 1997. A strong propagating disturbance associated with a CME was detected on 8 January when the radio ray path proximate point was on the east solar limb at about 32 solar radii from the Sun. Characteristics of the CME passage through the Galileo/Earth line of sight include: (a) a noticeable change of the average frequency of the radio signal, (b) a significant increase in the fluctuation level of the radio frequency and amplitude, and (c) a dual-velocity solar wind configuration with distinctly different values of the velocity (200 km/s and 360 km/s). These velocity estimates are obtained from a correlation analysis of frequency fluctuations recorded simultaneously at two widely-separated ground stations. The frequency fluctuation cross-correlation functions are relatively narrow during the passage of the disturbance through the radio ray paths, implying that the outward solar wind transport in the CME may be described as an ordered flow. The density turbulence power spectrum becomes steeper behind the CME leading front but becomes unusually flat near the trailing edge. It is shown that the effects observed in the Galileo radio-sounding data are associated with the same CME observed first (6 January) by the SOHO/LASCO coronagraphs near the Sun and later (10–11 January) in the solar wind on the WIND spacecraft near the Earth (e.g. abrupt changes in ion density, peaks in the velocity, interplanetary magnetic field enhancements).

Keywords: Solar corona; Radio sounding; Coronal mass ejection; Galileo spacecraft

1. Introduction

A coronal mass ejection (CME) in the inner heliosphere can propagate with very high velocities and is usually characterized by enhanced densities and temperatures. Upon encountering the Earth, these phenomena can deform the magnetosphere, trigger magnetic storms and pose a real danger for human activities in the terrestrial space environment.

The radio-sounding technique for the study of plasma disturbances in the solar wind has been exploited since the Pioneer-6 mission in 1968 [1, 2]. The radiometric parameters available for diagnostic investigations of CME-induced interplanetary disturbances during their passage

Astronomical and Astrophysical Transactions
ISSN 1055-6796 print/ISSN 1476-3540 online © 2007 Taylor & Francis
http://www.tandf.co.uk/journals
DOI: 10.1080/10556790701595210

through the radio propagation path include spectral broadening [1, 3, 4], Faraday rotation [2, 5], intensity scintillations [3, 6], and Doppler frequency fluctuations [7]. A large volume of experimental data has since been accumulated on many long-lived spacecraft missions during different phases of solar activity. A statistical analysis of radio-sounding observations with Pioneer Venus Orbiter over the period 1979–1987 made it possible to establish a number of typical features expected from solar wind plasma disturbances at different heliocentric distances and levels of solar activity [7]. In particular, a definite correlation could be formulated between the radio effects connected with the transients and coronagraph observations of the coronal mass ejections [8] or plasma measurements on board the spacecraft Helios-1 [9].

Further observational data on solar wind transient disturbances were obtained in the period 1994–2002 during eight superior conjunctions of the spacecraft Galileo. One strong propagating disturbance associated with a CME in early February 1997 was investigated using both remote-sensing data in the solar corona and *in situ* measurements near Earth. Radio propagation experiments carried out with the Galileo spacecraft have now provided additional valuable information about the properties of this CME in the intermediate heliocentric distance range between the solar corona and Earth. In particular, it was established that the density turbulence power spectrum becomes steeper behind the CME front [10].

Another interplanetary disturbance associated with a CME occurred in early January 1997. This event, which has been investigated using many remote-sensing methods as well as *in situ* measurements in interplanetary space and near the Earth [11, 12], is the subject of the present work.

2. The January 1997 CME

A coronal transient was first detected as a halo CME in the SOHO C2 coronagraph at 17:34 UT on 6 January 1997, i.e. at 006:17:34 UT (in the following all UT epochs will be denoted as doy:hh:mm, where doy is the day of year, and hh:mm is the time of day in hours and minutes). The propagation of the CME through the interplanetary medium was tracked remotely by the WAVES instrument on the WIND spacecraft through the detection of kilometric type II radio emissions, which are generated at the fundamental and harmonic of the plasma frequency by electrons accelerated at the interplanetary shock [12, 13]. Type II harmonic emission was observed on WIND at a distance of 90 R_S (solar radii) from the Sun at 008:02:00 UT.

The CME-driven shock was observed near the Earth on the WIND spacecraft starting at 010:01:00 UT. This time lag implies an average shock speed through the interplanetary medium of 500 km/s. The subsequent CME, which displayed the characteristics of a magnetic cloud, was observed from 010:05:00 UT to 011:01:00 UT. A radially outward propagating density pulse of up to 185 cm^{-3}, observed at about 011:01:00 UT, was the largest ever recorded in the solar wind at 1 AU [12]. Detailed analysis of this event suggests that the material originated from a solar prominence. The enhancement of the solar wind density caused global compressions of the magnetosphere, resulting in plasma sheet density enhancements, deep penetration of the plasma sheet into the near-Earth region, and other events [14].

Radio propagation experiments carried out in this period with the Galileo spacecraft at Jupiter provide additional information about the properties of this event. The characteristics of the plasma inside and outside the CME, including the level and shape of the turbulence spectrum, can be investigated with records of the radio frequency and amplitude fluctuations. A description of plasma effects on the observed frequency and its fluctuations is briefly reviewed for easier reference in the next section. Subsequent sections present the results derived from radio-sounding observations of the January 1997 CME with Galileo and a comparison with previously published WIND observations [12].

3. Frequency and amplitude variations in the turbulent solar wind

The frequency (phase) and amplitude of radio waves transmitted from interplanetary spacecraft are modulated by electron density irregularities in the solar wind plasma. We consider here the effects of large-scale plasma disturbances on the frequency of radio waves propagating through the interplanetary medium. The phase of a monochromatic wave with radio frequency $\omega_0 = 2\pi f_0$ is determined in the receiving station as

$$\Phi(t) = \omega_0 t - \frac{\omega_0}{c}\int_0^L n(z,t)dz \tag{1}$$

where c is the velocity of light; $n(z,t)$ is the refractive index, and the propagation path of length L is aligned with the z-axis. The instantaneous frequency, the time derivative of the phase, is

$$\omega = \mathrm{d}\Phi/\mathrm{d}t \tag{2}$$

The refractive index in a plasma is given by

$$n(z,t) = \left(1 - \frac{\omega_p^2}{\omega_0^2}\right)^{1/2} \tag{3}$$

where $\omega_p = \sqrt{4\pi N_e e^2/m}$ is the plasma frequency, $N_e(z,t)$ is the electron density, and e and m are the charge and mass of the electron, respectively.

If $\omega_p \gg \omega_0$, it is follows from (1), (2) and (3)

$$\omega = \omega_0\left(1 - \frac{v_z}{c}\right) + \lambda r_e \frac{d}{dt}\int_0^L N_e(z,t)dz, \tag{4}$$

where $r_e = e^2/mc^2$ is the classical electron radius, $\lambda = 2\pi c/\omega_0$ is the wavelength, and v_z is the spacecraft velocity projected along the ray path.

The value of the radial velocity v_z can be obtained from navigation data so that the classical Doppler shift term in (4) can be eliminated from the measurements. The fluctuating frequency residuals remaining after elimination of the regular Doppler shift are produced by plasma density irregularities along the ray path.

The effects of propagating plasma disturbances on the change of the average frequency have been considered for the cases of streamers and transients [15]. Here we analyse the random frequency fluctuations caused by turbulent electron density fluctuations superposed on the ambient background during the passage of a CME. In this case the plasma density can be considered to consist of two components:

$$N(z,t) = \langle N(z,t)\rangle + \delta N(z,t) \tag{5}$$

The ambient component $\langle N(z,t)\rangle$ changes with a characteristic time scale that exceeds the averaging time; the fluctuating component $\delta N(z,t)$ is a random function with an average value of zero. Let us suppose further that a disturbance produces an excess of the average electron density by $\langle N_{dis}\rangle$ above the background value $\langle N_{bg}\rangle$ such that $N(z,t) = \langle N_{dis}\rangle - \langle N_{bg}\rangle \approx \langle N_{dis}\rangle$ and that the disturbance moves transverse to the ray path at the velocity v_{dis}. If the physical dimensions of the disturbance are $\Lambda_{||}$ and $\Lambda_{\perp}$ along ray path and across ray path,

respectively, then the large-scale change of the radio frequency $\Delta\omega = \omega - \omega_0$ arising from the electron density excess can be estimated from (4) as

$$\Delta\omega = 2\pi\,\Delta F = (\lambda r_e) v_{dis} \langle N_{dis} \rangle (\Lambda_{||}/\Lambda_{\perp}) \tag{6}$$

The moving electron density irregularities in the disturbance will also produce a change in the random frequency fluctuations. In the following we assume that the spatial spectrum of the density fluctuations in the inertial interval $\Phi_{\mathrm{N}}(q)$ is an isotropic power law of the form

$$\Phi_{\mathrm{N}}(q, r) = C_{\mathrm{N}}(r)(q^2 + q_0^2)^{-p/2} \exp(-q^2/q_m^2) \tag{7}$$

with a 3-D spectral index p, an inverse turbulence outer scale q_0, an inverse turbulence inner scale q_m and a structure constant C_N, which is related to the electron density variance $\langle \sigma_N^2 \rangle$ by

$$\mathrm{C}_N(r) = \frac{(p-3)\langle \sigma_N^2(r) \rangle \Gamma(p/2) q_0^{\mathrm{p}-3}(r)}{(2\pi)^{3/2}\Gamma[(p-1)/2]} \tag{8}$$

where $\Gamma(\mathrm{x})$ is the Gamma function. The temporal power spectrum of the frequency fluctuations $G_f(\nu)$ can be expressed by [16]:

$$\mathrm{G_f}(v) = \alpha \cdot 2^{-\alpha}\pi^{-1-\alpha}(\mathrm{r_e}\lambda)^2 \sigma_{\mathrm{N}}^2 \mathrm{L_{eff}}\, v^{\alpha+1} \mathrm{q}_0^{\alpha} \cdot \nu^{-\alpha} \exp(-\nu^2/\nu_{\mathrm{m}}^2) \tag{9}$$

where v is the velocity of the medium projected perpendicular to the ray path, ν is the fluctuation frequency, ν_m is the fluctuation frequency corresponding to the inner scale of turbulence, $\nu_m = v q_m/2\pi$, and L_{eff} is the effective thickness of the modulating turbulent layer. Under quiet conditions, when the plasma flow is approximately symmetric, the scattering layer is centered on the ray path's proximate point to the Sun and has a thickness $L_{\mathrm{eff}} \approx R$. If the main modulation is caused by a large-scale disturbance, then L_{eff} is equal approximately to its longitudinal scale $\Lambda_{||}$. The relation (9) shows that the frequency fluctuation power spectrum is a power law with spectral index $\alpha = p - 3$. Integrating (9) over the fluctuation frequency ν from ν_0 to some maximum frequency ν_{max} yields the frequency variance $\langle \sigma_f^2 \rangle$. If the Nyquist frequency ν_{N} is substantially less than the frequency ν_m, then $\nu_{max} = \nu_{\mathrm{N}}$ and the frequency variance can be expressed by the following relation:

$$\langle \sigma_{\mathrm{f}}^2 \rangle = [\alpha/(1-\alpha)]\, 2^{-\alpha}\pi^{-1-\alpha}(\mathrm{r_e}\lambda)^2 \sigma_{\mathrm{N}}^2 \mathrm{L_{eff}}\, v^{\alpha+1} \mathrm{q}_0^{\alpha} \cdot \nu_{\mathrm{N}}^{1-\alpha} \tag{10}$$

which shows that $\langle \sigma_f^2 \rangle$ is proportional to both the electron density variance $\langle \sigma_{\mathrm{N}}^2 \rangle$ and the projected solar wind velocity v.

From (6) and (10) it follows that

$$\sigma_{\mathrm{f}}/\Delta F = (\sigma_{\mathrm{N}}/\langle \mathrm{N_{dis}} \rangle)(\nu_{\mathrm{N}}/q_0 v)^{(4-p)/2} (q_0/\Lambda_{||})^{1/2} \Lambda_{\perp}, \tag{11}$$

if $v \approx v_{dis}$.

This relation allows us to estimate the normalized level of turbulence $\sigma_N/\langle N_{dis} \rangle$ behind the disturbance front, provided one has independent information on the parameters p and q_0. It is reasonable to suggest that the parallel and perpendicular dimensions $\Lambda_{||}$ and $\Lambda_{\perp}$ are probably about the same. An interesting situation arises for the case of steep turbulence spectra with $p \approx 4.0$. The relation (11) then depends only weakly on the velocity v and the outer turbulence scale q_0.

4. Observations and data processing

Coronal radio-sounding experiments were conducted using the radio signal of the Galileo spacecraft during its recurring solar conjunctions. The downlink S-band signal (carrier frequency: 2.295 GHz; $\lambda = 13.1$ cm) was generated by an ultra-stable oscillator with extremely high frequency stability. The Allan variance of the transmitted signal frequency was many times lower than the typical frequency variance imposed on the signal during its passage through the outer solar corona. The radio signals were recorded with a sampling rate of 1 Hz at three 70-m NASA DSN tracking stations Canberra (DSS 43), Madrid (DSS 63) and Goldstone (DSS 14). Doppler residuals for each tracking pass were calculated by subtracting a slowly varying frequency component from the raw data to compensate for the spacecraft motion relative to the observer.

The Doppler residuals recorded on the days 7–12 January 1997 are presented in figure 1 for all three tracking stations: DSS 63 (green trace), DSS 14 (red trace) and DSS 43 (black trace). During this period the Galileo/Earth radio ray path was east of the Sun at a geometric proximate heliocentric distance R that decreased from 37.4 to 21.0 R_S. Figure 1 describes the general trend in the frequency residuals over this period. It is seen that there is linear increase of the average frequency (from 0.4 up to 0.5 Hz) which probably is associated with the spacecraft oscillator. Another feature is an increase of the frequency fluctuations as the Galileo/Earth radio ray path approaches to the Sun. The radio tracking configuration at all stations was one-way (downlink only).

Figure 1 clearly reveals the onset of the event on 8 January 1997 as a sharp increase in the average radio frequency beginning at 17:05 UT and lasting for approximately three hours. The mean frequency returned rather smoothly to its undisturbed level in the time interval from 20:10 to 20:28 UT. The proximate heliocentric distance of the Galileo/Earth radio ray path at this time was $R \approx 32 R_S$. Observations of this interesting event were carried out at DSS 14 for most of the period (008:16:09 to 009:00:52 UT) and for smaller segments at DSS 63 (008:13:27 to 008:16:32 UT) and DSS 43 (008:20:39 to 009:09:05 UT). A more detailed plot of the Doppler residuals recorded near the event is presented in figure 2. Simultaneous measurements at two widely-spaced ground stations were obtained in two overlap intervals: DSS 63/14

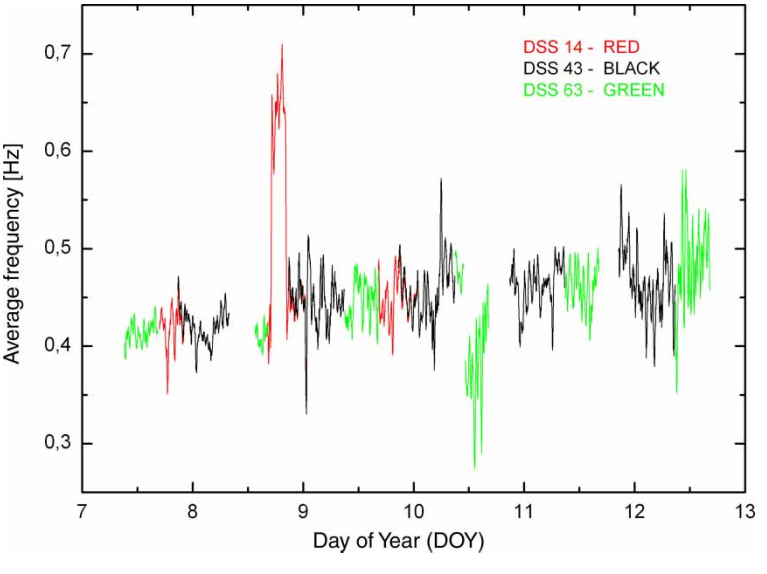

Figure 1. Galileo Doppler residuals recorded during the period 7–12 January 1997.

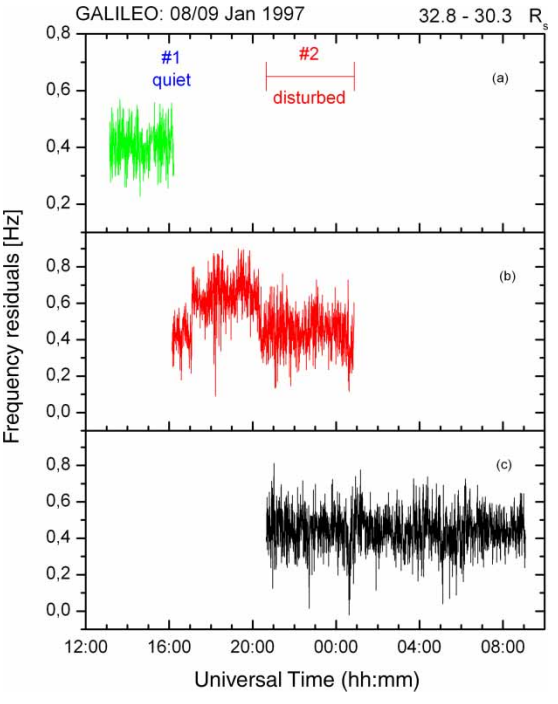

Figure 2. Galileo Doppler residuals recorded near the passage of a coronal mass ejection at DSS 63 (upper curve), DSS 14 (middle) and DSS 43 (lower). The abrupt increase in average radio frequency at 008:17:05 UT is interpreted as the initial passage of a disturbance (leading edge of an interplanetary CME) into the Galileo signal ray path.

(#1, 008:16:09-008:16:32 UT) in a period of rather quiet conditions, and DSS 14/43 (#2, 008:20:39-009:00:52 UT) in a period just following the passage of the CME disturbance through the radio ray path.

Temporal power spectra of the frequency fluctuations were calculated for the data of figure 2 using a standard FFT algorithm on successive subintervals of 4096 s. The falloff exponent α (spectral index) of each spectrum was determined in the spectral range 10^{-3} Hz $< 5 \cdot 10^{-2}$ Hz. The mean frequency fluctuation $\sigma_{\mathrm{f}} = \sqrt{\langle \sigma_{\mathrm{f}}^2 \rangle}$ was calculated directly from the Doppler record for each 4096 s interval. Frequency fluctuation cross-correlation functions were calculated for the overlap intervals. The projected speed of the modulating irregularities $v_\perp$ was found as the ratio of the calculated two-station ray path radial separation ΔR to the time lag τ_m of maximum frequency cross-correlation between the two stations:

$$v_\perp = \Delta R / \tau_m \tag{12}$$

Noting that the solar wind velocity greatly exceeds both the Alfvén velocity and the speed of sound at the heliocentric distance $R \approx 32 R_{\mathrm{S}}$, we can assume that the speed of the irregularities is approximately equal to the solar wind flow speed projected perpendicular to the line of sight. Temporal frequency fluctuation spectra were calculated separately for both stations in all overlapping intervals. No significant difference in the mean frequency fluctuation σ_f or spectral index α could be found from a comparison of the data from each station.

Intensity fluctuations were calculated using a technique applied earlier to Ulysses measurements [17]. The raw experimental data, which were expressed in dB above a given level, were transformed into normalized intensity residuals with respect to their average value I_0. Unfortunately, more quantitative information on the high frequency part of the temporal fluctuation spectra is unavailable because of the rather low sampling rate of 1 Hz. However, it is

still possible to study fluctuations at higher spectral density levels and calculate the variance of the intensity fluctuations with periods larger than 1 second.

5. Characteristics of the frequency and intensity variations

Results of the frequency fluctuation spectral analysis for the data associated with the event are presented in figure 3(a) and (b). Changes in the level of the mean frequency fluctuation σ_f resulting from the transit of the disturbance through the radio ray path are illustrated in figure 3(a). An increase of the frequency fluctuations by a factor of three was observed within one hour after the sharp increase in average frequency at 17:05 UT. The fluctuation level decreased slightly during the decrease of the average frequency to its pre-event level (at about 008:20:20 UT), but maintained an enhanced value with respect to the quiet period up to 009:08:30 UT.

The temporal evolution of the spectral index α(t) is presented in figure 3(b). Values of the spectral index before the arrival of the disturbance were $\alpha \approx 0.7$, corresponding to Kolmogorov turbulence. Upon passage of the leading front of the disturbance, the spectral index increased to $\alpha \approx 1.0$, simultaneously with the increase of the mean frequency fluctuation σ_f. After the decrease of the average frequency of the signals was detected at the ground station DSS 14 (passage of a trailing CME front?), the spectral index α_f decreased to an anomalously low value $\alpha \approx 0.35$. This low value was then retained for several hours. A second increase in the spectral index was observed at about 009:02:00 UT, after which the values of α varied within the usual range between 0.55 and 0.75.

The data presented in figure 3(a) and (b) imply good correlation between the variations of σ_f and α during the passage of the disturbance through the ray path – the enhancement of the frequency fluctuations is directly followed by an increase of the spectral index. Generally, the spectral index varies over a wide range (from 0.35 to 1.1) during all observation periods, but there is a tendency for an increase of α and enhancement of σ_f connected with passage of the disturbance.

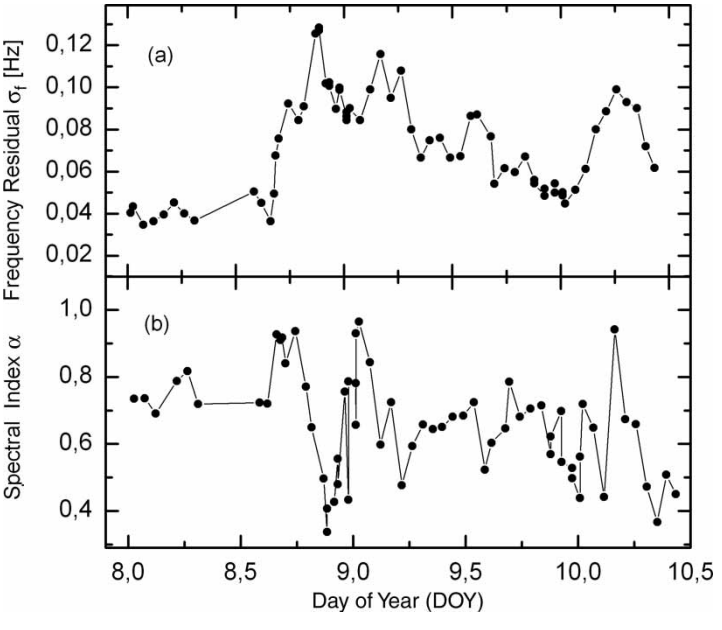

Figure 3. Characteristics of the frequency fluctuations during the passage of the CME through the radio ray path Galileo/Earth. Panel (a): RMS Doppler fluctuation level. Panel (b): Frequency fluctuation spectral index.

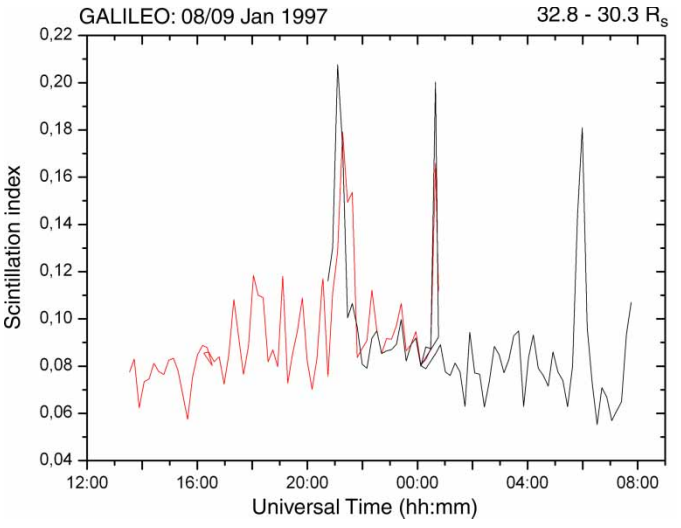

Figure 4. RMS intensity fluctuation level during the passage of the CME through the radio ray path Galileo/Earth.

Figure 4 presents the temporal dependence of the RMS intensity fluctuation $\langle \Delta I \rangle$, normalized to the average value of the intensity I_0, during the event. Each point is generated from five individual FFT-128 spectra. These ratios, $\langle \Delta I \rangle / I_0$, are similar to the scintillation index m, which is commonly used for estimating the intensity fluctuation level of a radio signal. The difference is that m is defined for fluctuations at all frequencies, not just those below 1 Hz, so that m is always greater than $\langle \Delta I \rangle / I_0$. The times of the intensity fluctuation enhancements in figure 4 are observed to be coincident with the increases in frequency fluctuations recorded at the ground stations (figure 3(a)).

The cross-correlation function of frequency fluctuations measured simultaneously at the two ground stations DSS 14/63 is shown in the upper panel of figure 5 for the overlap interval #1 (quiet conditions). Rather slow solar wind was observed during this period. The time lag of maximum cross-correlation was $\tau_m = 27.5$ s for the radial radio ray path separation of $\Delta R = 7064$ km. The corresponding convective projected speed from (12) is $v_\perp = 257$ km/s and the solar wind velocity $v = v_\perp - v_{raypath} = 257 - 22$ km/s $= 235$ km/s.

The lower panel of figure 5 shows the cross-correlation function calculated from simultaneous Doppler recordings at DSS 14/43 in the disturbed (CME) overlap interval #2. Two peaks are seen at the lag times $\tau_{m1} = 16.4$ s and $\tau_{m2} = 28.5$ s. Using the radial separation for this case, $\Delta R = 6202$ km, the convective velocities are found to be 378 km/s and 218 km/s, respectively. The corresponding values of the solar wind velocities are $v_1 = 356$ km/s and $v_2 = 196$ km/s. It is suggested that the two velocities correspond to the undisturbed solar wind with maximum plasma content near the ray path proximate point to the Sun (v_2) and a different region within the propagating disturbance (v_1) with maximum electron density between the proximate point and the observer. This hypothesis is consistent with the small difference between the velocity v_2 and the velocity measured earlier under quiet conditions (figure 5 – upper panel).

6. Comparison with SOHO/LASCO and wind data

The leading edge of an energetic CME was observed in white light by the SOHO/LASCO C2 coronagraph starting from 006:17:34 UT at a heliocentric distance $R \approx 3.7 R_S$. The CME

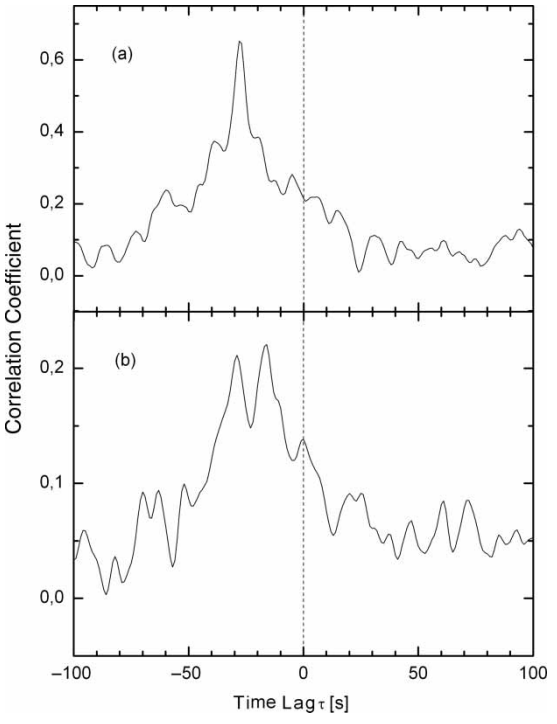

Figure 5. Cross-correlation functions in station overlap intervals: Panel (a): DSS 63/14, quiet, overlap interval #1. Panel (b): DSS 14/43, disturbed (CME), overlap interval #2.

frontal structure crossed the Galileo/Earth ray path at about 008:17:05 UT, implying a time delay between events near the Sun and on the ray path is about of 47.5 hours. Since the exact position of the disturbance is not known, it may only be deduced that the distance travelled by the CME is $r > R$, where the solar offset $R \approx 32R_S$. The convection velocity $v_\perp$ transverse to the ray path determined from the two-station frequency fluctuation cross-correlation function is assumed to be related to the true disturbance speed v_{dis} by

$$v_\perp = v_{dis}\, R/r. \tag{13}$$

If the time delay of the disturbance arrival relative to its sighting in the solar corona is ΔT, then its average speed is determined by relation $v_{dis} = r/\Delta T$. Taking (13) into consideration, we obtain $v_\perp = R/\Delta T = 115\,\mathrm{km/s}$ for $R = 32R_S$ and $\Delta T = 47.5$ hours. This value is substantially less than the velocity obtained from the cross-correlation analysis $v_1 = 356\,\mathrm{km/s}$. Possible causes of this difference are (a) an acceleration of the disturbance or (b) a projection effect of the local fluctuation velocities, which can be substantially higher than in the mean solar wind speed behind the disturbance front.

Figure 6 presents a comparison of the temporal dependence of the average frequency of the Galileo signal (upper panel) with the average values of the plasma density near the Earth's orbit using the WIND spacecraft (lower panel). A huge increase in the solar wind plasma density was seen by WIND at 011:00:30 UT that lasted for three hours and then relaxed quickly to a value corresponding to undisturbed conditions. Comparing the onset of this event with the time of the increase in frequency fluctuations (008:17:05 UT at $R > 32R_S$), we find that the time delay is about 55 hours. Noting that the distance travelled by the disturbance during this time must be less than 181 R_S, we can find an upper bound on the transit speed of the CME front of $\langle v_{dis} \rangle < 630\,\mathrm{km/s}$ ($32R_S < R <$ 1AU). This is in good agreement with

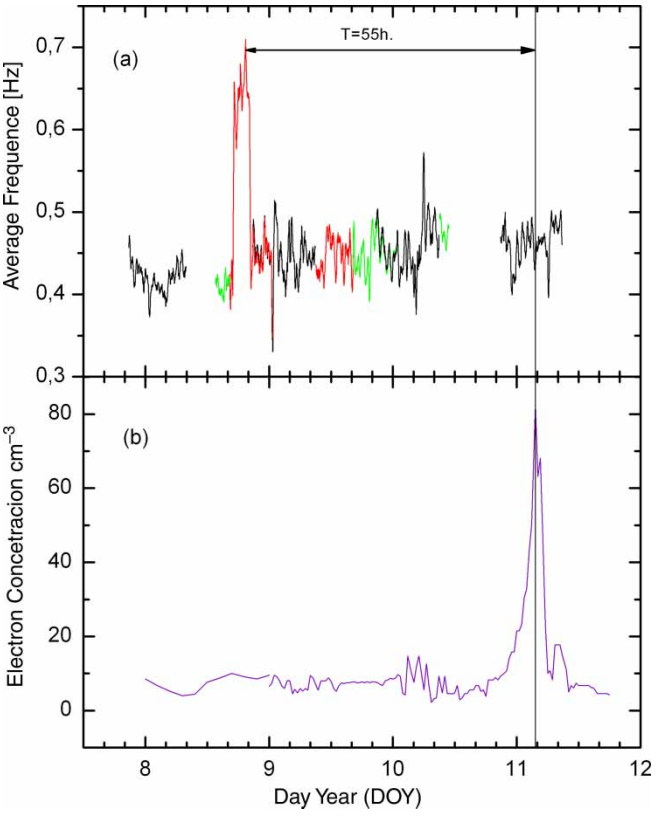

Figure 6. Doppler residuals (upper panel) and electron density of the solar wind near the Earth (lower panel) recorded during the period 7–11 January 1997 [12].

the measured cross-correlation value v_1 and the velocity of the disturbed solar wind near the Earth $v_{dis} \approx 520\,\mathrm{km/s}$ measured *in situ* on WIND.

Using relation (6) we can now estimate the maximum plasma density in the disturbed solar wind $\langle N_{dis} \rangle$ at the heliocentric distance 32 R_S on the assumption that $\Lambda_{||} = \Lambda_{\perp}$ and $v_{dis} = 500\,\mathrm{km/s}$. In this case the observed frequency shift $\Delta F \approx 0.3\,\mathrm{Hz}$ yields $\langle N_{dis} \rangle \approx 1.02 \times 10^4\,\mathrm{cm}^{-3}$. This may be compared to the average background density of the solar wind plasma at $32 R_S$, $\langle N_{bg} \rangle \approx 5 \times 10^2\,\mathrm{cm}^{-3}$. The maximum solar wind plasma density in the CME is thus 20–30 times larger than the mean ambient density. This conclusion is supported by the *in situ* measurements on WIND (figure 6 – lower panel).

7. Conclusions

Continuous monitoring of radio signals from spacecraft near superior solar conjunction is a useful tool for detection and analysis of CMEs in the inner solar wind. The passage of a CME through the Earth/spacecraft radio ray path induces a characteristic signature on the radio signals. The first effect is a strong enhancement of the fluctuations in frequency and amplitude that can last for many hours. Another effect is an increase in the slope of the turbulence power spectrum behind the CME front. Finally, an increase in the average radio frequency can be detected upon passage of a high density plasma flow with a steep density gradient. These effects provide clues about the solar wind plasma turbulence and outflow

regimes generated by coronal mass ejections. Specific conclusions drawn from the Galileo radio-sounding observations of the January 1997 CME at $32R_S$ are as follows:

1. The effects on the radio signal during passage of the CME through the line-of-sight:
   - enhanced intensity of the frequency and amplitude fluctuations by a factor of 2–3;
   - enhanced value of the frequency fluctuation spectral index behind the CME leading edge;
   - unusually low value of the spectral index after passage of the CME leading edge;
   - increase in the average signal frequency;
   - double maxima in the frequency fluctuation cross-correlation function.
2. The maximum plasma density in the CME leading edge exceeds the background value by more than an order of magnitude.
3. The appearance of two maxima in the frequency fluctuation cross-correlation function implies the presence of separate quiet and disturbed flows along the line-of-sight with different maximum plasma density and turbulence levels.
4. The CME on the east solar limb was observed in Galileo radio-sounding data more than two days prior to its detection near the Earth.

Acknowledgements

The present work was supported by the Programme 'Plasma Processes in the Solar System' of the Russian Academy of Sciences and by Grant 04-02-17332 of the Russian Foundation of Basic Research (RFBR). This paper presents result of research partly funded by the Deutsche Forschungsgemeinschaft (DFG) under a cooperative program between the DFG and RFBR (Grant 05-02-04002). The authors wish to express their gratitude for the continued support of the Galileo Project, the Multi-Mission Radio Science Team and the NASA Deep Space Network.

References

[1] R.M. Goldstein, Science **166** 598 (1969).
[2] G.S. Levy, T. Sato, B.L. Seidel, C.T. Stelzried, J.E. Ohlson and W.V.T. Rusch, Science **166** 596 (1969).
[3] R. Woo and J.W. Armstrong, Nature **292** 608 (1981).
[4] R. Woo and J.W. Armstrong, J. Geophys. Res. **84** 7288 (1979).
[5] M.K. Bird, H. Volland, R.A. Howard, M.J. Koomen, D.J. Michels, N.R. Sheeley, J.W. Armstrong, B.L. Seidel, C.T. Stelzried and R. Woo, Solar Phys. **98** 341 (1985).
[6] J.W. Armstrong and R. Woo, Astron. Astrophys. **103** 415 (1981).
[7] R. Woo, J. Geophys. Res. **93** 3919 (1988).
[8] R. Woo, J.W. Armstrong, N.R. Sheeley and M.J. Koomen, J. Geophys. Res. **90** 154 (1985).
[9] R. Woo and R. Schwenn, J. Geophys. Res. **96** 227 (1991).
[10] A.I. Efimov, L.N. Samoznaev, I.V. Chashei, M.K. Bird and D. Plettemeier, Radiotekhnika **12** 36 (2005) (in Russian).
[11] G. Le, C.T. Russell and J.G. Luhman, Geophys. Res. Lett. **25** 2533 (1998).
[12] N.J. Fox, M. Peredo and B.J. Thompson, Geophys. Res. Lett. **25** 2461 (1998).
[13] M.J. Reiner, M.L. Kaiser, J. Fainberg, J.L. Bougeret and R.G. Stone, Geophys. Res. Lett. **25** 2493 (1998).
[14] M.F. Thomson, J.E. Borovsky, D.J. McComas, R.C. Elphic and S. Maurice, Geophys. Res. Lett. **25** 2545 (1998).
[15] G.G. Dolbezhev, A.I. Efimov, V.F. Tikhonov and O.I. Yakovlev, J. Commun. Technol. Electron. **31** 125 (1986).
[16] N.A. Armand, A.I. Efimov, L.N. Samoznaev, M.K. Bird, P. Edenhofer, D. Plettemeier and R. Wohlmuth, J. Commun. Technol. Electron. **48** 970 (2003).
[17] A.I. Efimov, M.K. Bird, V.K. Rudash, V.E .Andreev, I.V. Chashei, D. Plettemeier and P. Edenhofer, Adv. Space Res. **35** 2189 (2005).